

Using cellular automata to simulate field-scale flaming and smouldering wildfires in tropical peatlands

Dwi M J Purnomo^a, Matthew Bonner^a, Samaneh Moafi^b,
Guillermo Rein^{a,*}

^a *Leverhulme Centre for Wildfires, Environment and Society, and Department of Mechanical Engineering, Imperial College London, London SW7 2AZ, United Kingdom*

^b *Forensic Architecture, Goldsmiths, University of London, London SE14 6NW, United Kingdom*

Received 7 November 2019; accepted 23 August 2020

Available online 30 October 2020

Abstract

Peat wildfires are the largest fires on Earth involving both flaming and smouldering combustion, with one leading to the other. A common ignition source of smouldering fires in tropical peatlands are intentional flaming fires used to clear surface vegetation. To capture the behaviour of these fires, it is necessary to consider the interaction between flaming vegetation and smouldering peat. However, doing so is infeasible with the state-of-the-art wildfire models, as they do not consider the transition from flaming to smouldering and are computationally too expensive at the field-scale hundreds of hectares. In this work, we overcome these limitations and model both flaming and smouldering at the field-scale using cellular automata: that is a discrete mathematical model that uses simple rules to capture complex behaviour while remaining computationally light. The model was calibrated against existing experiments in the literature and used to predict the effect of peat moisture content on the behaviour of peatland wildfires. The model shows how flaming creates smouldering hotspots and how these hotspots merge – flaming spreads rapidly, consuming surface vegetation, leaving behind hotspots of smouldering peat which consumes most of the peat. The model was then applied to study a real prescribed fire of 573 ha peatland in Borneo in 2015, observed by drone footage. The model captured the spread patterns of the fire and predicted that 2.9 ha of peatland burnt after 3 months with 70% peat moisture content (dry-based). This outcome could have been reduced to 0.02 ha if the peat moisture content had been above 100%. This work improves the fundamental understanding of how peat wildfires spread at the field scale which has received little attention until now.

© 2020 The Author(s). Published by Elsevier Inc. on behalf of The Combustion Institute.

This is an open access article under the CC BY license (<http://creativecommons.org/licenses/by/4.0/>)

Keywords: Prescribed fire; Modelling; Smouldering; Peat fire; Cellular automata

* Corresponding author.

E-mail address: g.rein@imperial.ac.uk (G. Rein).

1. Introduction

Smouldering peat wildfires are the largest and one of the most persistent fires in nature [1]. Every year, peat wildfires burn for weeks, producing large amounts of harmful emissions. Smouldering is a flameless form of combustion that spreads slower and have lower temperature than flaming combustion [2,3]. Natural causes (e.g. lightning) could start peat wildfires, however, a common ignition source for peat wildfires is the intentional burning of surface vegetation on peatland, either to clear land for farming or to prevent the build-up of fuel [4–6]. Despite these common practices, studies of prescribed fires on peatland are limited [7,8], and none of them have addressed the smouldering fire that often persist in the soil after the initial flaming fire ceases.

Part of the reason for the lack of attention on this fire is the complexity involved in considering both flaming and smouldering fires simultaneously. Smouldering could transition to flaming and vice versa, however, previous studies tended to only focus on the former [9]. Therefore, there is little knowledge of the most common cause of smouldering peat wildfires: ignition from a flaming fire along surface vegetation.

Considering these complex phenomena at the field-scale, using state-of-the-art wildfire models to simulate peat wildfires would be infeasible, as they cannot couple flaming and smouldering. Meanwhile, physics-based computational models (e.g. computational fluid dynamics (CFD)) are computationally too expensive to simulate peat wildfires at the field-scale (hundreds of hectares of area). In this paper, we consider an alternative method: Cellular Automata [10,11]. This simpler model considers a grid of cells that can be in different states (e.g. fuel, burning, residue). The state of each cell can then update itself over discrete time-steps using either deterministic or stochastic rules. By considering simple rules rather than complex physical interactions, cellular automata are much more computationally efficient than physics-based models (e.g. CFD). This computational efficiency refers to the number of instructions a computer would need to execute, with efficient models requiring fewer instructions (and thus fewer resources) to achieve a similar result.

Cellular automata have been used to simulate both flaming wildfires [12–14] and smouldering combustion in peat [15,16], however, this paper is the first time cellular automata have been applied to field-scale peat wildfires and includes both flaming vegetation and smouldering peat, as well as the transition between them. The model is used to investigate the effect of the moisture content (MC) of peat on fire spread, first in a uniform fuel grid, and then in a real prescribed fire in tropical peatland in Borneo.

2. Methods

2.1. Cellular automata

Cellular Automata (CA) are discrete computational models that use simple rules to simulate complex emergent behaviour [10,11]. These models use a finite $m \times n$ grid of cells, each of which can be in one of k discrete states – essentially a form of matrix. This grid updates itself over discrete time-steps. At each time-step, every cell in the grid will update its state based on a set of rules according to other nearby cells (*neighbourhood*). By choosing representative states and rules, these abstract models can simulate complex physical phenomena.

One set of phenomena that have been modelled using CA are wildfires. Different states and update rules have been chosen for these CA, depending on what aspects of the fires (e.g. fire spread behaviour) should be captured, for example, in [13–16]. In this work, we aim to create the simplest model that could still adequately capture the behaviour seen in peatland fires involving flaming and smouldering combustion. Inspired by previous CA studies, we chose the method called *bond percolation*. *Bond percolation* has been used to implement different aspects of wildfires in CA models [17]. This method deals with the existence of connections (bonds) between an entity and its surrounding. In practice this method can be applied to wildfires, where the connections in *bond percolation* represent the flammability of the surrounding fuels when they are consumed by the fire. Percolation principle stems from non-exact phase transition [14], therefore, the existence of these connections are stochastic (they occur with some probability less than 1). This stochastic approach is also relevant to the real wildfires due to the uncertainty of nature, for example, caused by landscape heterogeneity. In the model, an unburned cell will update itself to a burning cell with a probability P if there are other burning cells in its neighbourhood. The most used neighbourhood in the literature was chosen, known as a Moore neighbourhood – the eight cells directly surrounding the considered cell in a 3×3 square grid. From here on, we will refer to the model in this work as KAPAS.

2.2. States and rules of the model

KAPAS considers 5 possible states for each cell: *surface vegetation (SV)*, *flaming vegetation (FV)*, *exposed peat (EP)*, *smouldering peat (SP)*, and *burned peat (BP)* (see Fig. 1). *EP* represents a cell which has lost its surface vegetation, due to flaming, but the peat underneath it remains intact since the smouldering has not started. These states represent the smallest number of states that can still capture the interaction between flaming and smouldering of two fuel types in peatlands. For simplicity, we did not consider the possibility of flaming peat

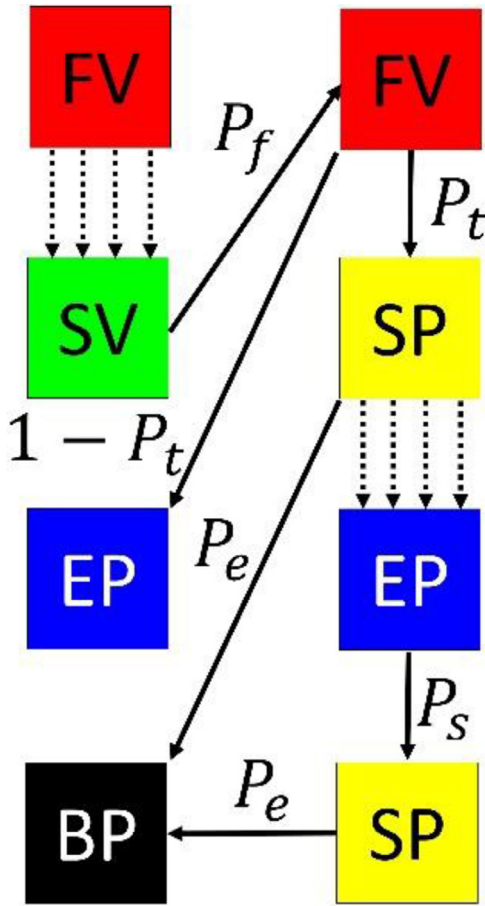


Fig. 1. The states and rules of the model. SV is surface vegetation, FV is flaming vegetation, EP is exposed peat, SP is smouldering peat, BP is burned peat, and P_x are probabilities of state change. Solid arrows represent state change, whereas dotted arrows represent the influence from neighbouring cells.

in this work because it happens rarely [2]. KAPAS is initiated at $t = 0$ by igniting particular cells (i.e. changing from SV to FV). These FV cells will update their states after one time-step (following the work in [17]) to either EP or SP, based on the probability of transition between flaming and smouldering P_t . Surface vegetation mass is limited compared to peat deposits and burns much faster with flaming [2], therefore, FV has a 100% chance to transition to EP or SP. SV cells nearby any FV cell may become FV cells with probability P_f . EP cells nearby any SP cell may become SP cells with probability P_s . Finally, SP cells have a probability of extinguishing to become BP cells, with probability P_e . KAPAS also considers the surface vegetation and peat as 2 separate layers of cellular automata, meaning that smouldering can spread to nearby peat even if

there is still surface vegetation above. This multi-layer approach was inspired by [16].

The ability of KAPAS to represent coupling between flaming and smouldering combustion in peatlands depend on the choice of the four parameters P_f , P_t , P_s , and P_e . Such parameters are often found by fitting to a particular fire, however, in this work they were chosen based on many different sources and experimental studies, allowing the model to be more general in principle.

2.3. Selecting parameter values

The flame spread probability P_f was chosen by finding a base probability P_R of flaming spread rate based on the Rothermel model for surface fire spread [18], augmented by a parameter representing the effect of wind, α_w . We use Rothermel spread rate (R) from [18] with a 0 m/s wind speed and its estimation can be found in appendix (see Eq. (A1)). P_R depends on both the cell size and time-step duration, as it is found by optimizing a probability that enable KAPAS to produce R as its spread rate when applied to a cell of Δx m in size and time-step Δt seconds over a large number of time-steps. In this work, with a cell size of 4.5 m and a time-step of 300 s, $P_R = 0.03$. We chose these cell size and time-step based on the highest resolution can be run with the available computing power.

P_R is then augmented by a wind parameter (α_w), following on from [17], which depends on the wind speed u , at around 6 m height above ground (weather station), and the angle between the fire propagation and the wind direction θ as shown in Eq. (1), where $c_1 = 0.045$ and $c_2 = 0.131$, following the work of [17]. The final probability of flame spread is then shown in Eq. (2), which means that each cell in the neighbourhood will have a different P_f depending on their relationship to the wind direction.

$$\alpha_w = e^{u(c_1 - c_2(1 - \cos\theta))} \tag{1}$$

$$P_f = P_R \cdot \alpha_w \tag{2}$$

Standard Rothermel model account for the wind effect, however, implementing this directly into KAPAS would significantly increase its computational cost, since P_R would need to be re-optimised every time the wind condition changed. For this reason, this method has never been used for bond percolation CA. By decoupling the wind effect as a separate parameter (P_f depends on P_R and α_w), KAPAS can simulate fires with different wind conditions in a computationally efficient way.

The probability of transition from flaming to smouldering P_t was found by adapting the work in [19], which investigated the smouldering ignition probability of peat based on its MC, inorganic content (IC), and bulk density (ρ). For simplicity, we only varied MC in this work, as this is the most im-

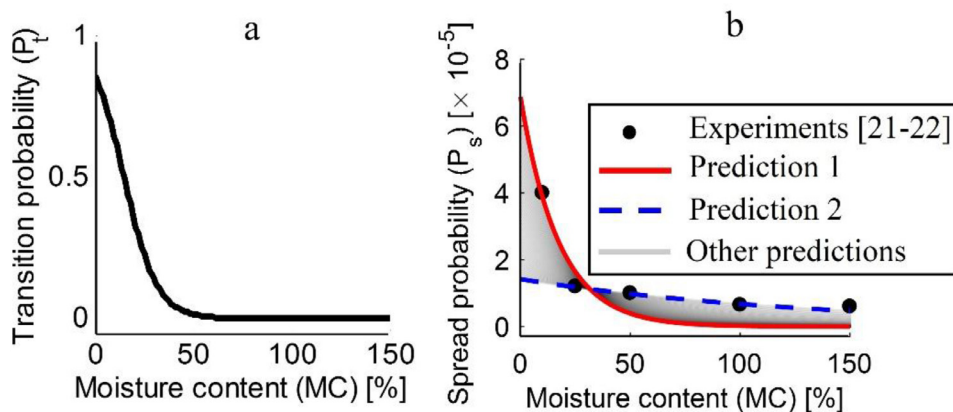


Fig. 2. Dependency on moisture content for (a) P_t and (b) P_s . The shape of these relationships are extracted from literature [19,21,22]. Prediction 1 uses $c_3 = 9.58$ and $c_4 = 0.057$, whereas prediction 2 uses $c_3 = 11.2$ and $c_4 = 0.006$.

portant property of peat for fire [3]. IC and ρ were set to 3.7% and 222 kg/m³ respectively [19,20]. This left P_t with a sigmoid relationship with respect to MC, shown in Fig. 2a.

The smouldering spread probability P_s was found by comparing smouldering spread rates taken from experiments on peat at different MC [21,22]. These spread rates are also given in cm/min, therefore, P_s depends on cell size and time-step duration, similar to P_R . These experiments used boreal peat, as studies on tropical peat are limited [23]. When MC, IC, and ρ have been considered, the resulting probabilities are expected to vary relatively little between tropical and boreal peats. Assuming P_s also has a sigmoid relationship (Eq. (3)) with respect to MC (similar to P_t) a variety of different curves could be fitted to the experiments considered, by changing c_3 and c_4 , as shown in Fig. 2b. The grey lines in Fig. 2b represent predictions which have good agreement with experiments. These plausible predictions are bounded by two polar opposite predictions, prediction 1 and 2. Prediction 1 has high accuracy for lower MC and low accuracy for higher MC, whereas prediction 2 is the opposite. Among the plausible predictions, we selected prediction 1 ($c_3 = 9.58$ and $c_4 = 0.057$) to determine P_s on a specific MC for KAPAS, because this prediction has the highest accuracy for peat with lower MC, which poses a greater hazard in fire.

$$P_s = \frac{1}{1 + e^{c_3 + c_4 MC}} \quad (3)$$

The smouldering extinction probability P_e was chosen based on the persistency of smouldering fire, i.e. once ignited, smouldering fires are very difficult to extinguish and will continue to burn for a long time [3]. These fires extinguish when they encounter a water table or mineral layer. In Indone-

sian peatlands, the peat layer is deep and the water table is low in dry season [24]. We chose these typical conditions (deep peat layer and low water table) in this work. Therefore, to make the smouldering fire remain active for a long time in KAPAS, P_e is set to be much lower than P_s . Setting P_e to be much lower than P_s means the smouldering fire remain active after the smouldering fire front has propagated relatively distant, which shows that the fire also has in-depth spread. Unfortunately, we found no previous work that could be used to derive P_e directly. Therefore, in this work, the value was chosen to be 5×10^{-7} to represent this persistency, an order of magnitude lower than P_s .

3. Results and discussion

3.1. Effect of moisture content in uniform fuel grid

We use KAPAS to explore the effect of MC on both smouldering spread and the transition from flaming to smouldering. We began by considering a uniform fuel grid (simplest case), completely filled with surface vegetation, and ignited in the centre (see Fig. A1). In the model, MC was varied from 0 to 150% in increments of 10%. KAPAS was run for a total duration of 10,000 time-steps (35 days in real time) in this first case. This total duration is selected since smouldering wildfires spread slowly and sustain for weeks [3]. The wind effect was ignored ($\alpha_w = 1$) in this first case, to isolate the effect of MC.

We use a grid of 400 × 400 cells grid (representing 324 ha) in this uniform fuel grid. We use this large grid size to avoid the finite size effect and minimize the uncertainty. Based on a sensitivity analysis, shown in Fig. A2, the burnt ratios (ϕ_b) and their standard deviations (from 10 simulation repe-

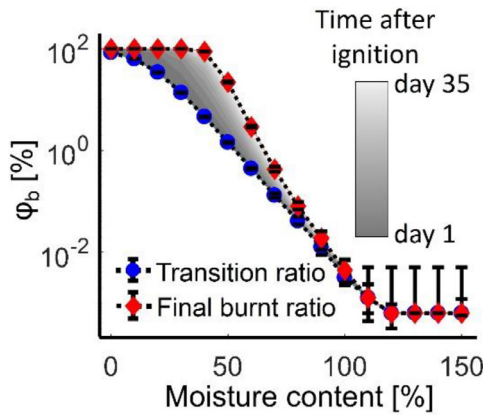


Fig. 3. Predicted φ_b for different moisture contents. The colour gradation represents φ_b every 3.5 days (1000 time steps). Each simulation is repeated 50 times to report uncertainty (error bars) and the averages are shown (symbols and colour bar). (For interpretation of the references to colour in this figure, the reader is referred to the web version of this article.)

titions) do not differ significantly once the grid size is larger than 400 x 400 cells. φ_b is calculated as the sum of *smouldering peat (SP)* and *burned peat (BP)* cells in the peat layer, divided by the total number of cells in the grid (i.e. area of the grid burned/total area of the grid). We also did sensitivity analysis on P_f as shown in Fig. A3. This analysis shows that P_f does not significantly affect φ_b and their uncertainties.

Figure 3 shows φ_b at every 3.5 day (1000 time-steps) after flaming ignition with increasing peat MC for IC of 3.7%. The line fitted through the blue circles represents φ_b immediately after all surface vegetation has been consumed, which only considers cells ignited from the transition from flaming to smouldering (P_f). We refer to this as the *transition ratio*. The line fitted through the red diamonds represents the final φ_b after 35 days. This is the *final burnt ratio*. The error bar in both transition and final burnt ratio represent the uncertainties of the simulation which are repeated 50 times for each MC.

The transition ratio follows a sigmoid relationship with MC, as would be expected from its dependence on P_f . This curve deviates from the ignition probability in [19] on average by 5.3%. KAPAS, therefore, demonstrates a novel way to augment the findings for ignition of smouldering of [19] (igniting peat with a metal coil) in the context of real wildfires. The final burnt ratio also follows a sigmoid relationship with respect to MC, which might be expected from the relationship of P_s . However, the shape of this sigmoid is significantly different from the sigmoid of the relationship between P_s and MC (see Fig. 2b). Therefore, there are important interactions between the smouldering and

flaming layers of the model, demonstrating the value of considering both layers.

Figure 4 shows the evolution of burnt ratio with time for 3 different MC values. The burnt ratio change ($\Delta\varphi_b$) is equal to the current value of φ_b minus the value of φ_b 3.5 day earlier. If the peat was ignited at the centre and allowed to spread with no interaction with the flaming vegetation, then $\Delta\varphi_b$ would increase linearly with time as the smouldering fire grew simply from one single hotspot. However, Fig. 4 demonstrates that in the multi-layer model this linear growth only happens at high MC. At lower MC, $\Delta\varphi_b$ decreases with time after an initial increase. This decrease is caused by separate areas of smouldering peat (hotspots) merging. If the simulation at 10% and 30% MC was allowed to run indefinitely in an infinite grid, then eventually $\Delta\varphi_b$ would again start to increase linearly once all the hotspots had merged. In a real wildfire, this merging behaviour represents the point at which the fire is much harder to fight, as this phenomenon disables the safe routes for firefighting, whereas water bombing effectiveness against smouldering peat is questionable. Fig. A4 shows an example of a merging phenomenon in real peat wildfires in Sumatra, Indonesia in 2019.

KAPAS shows that a wildfire on peatlands with MC above 120% has transition and final burnt ratio converge to zero. Therefore, this peatland condition would be relatively safe for performing prescribed fires. KAPAS also demonstrates hotspots initiation by flaming vegetation and how complex behaviour (hotspots merging) can emerge from a simple rule-based model.

The MC threshold for a safe prescribed fire according to the model conforms to the experiments in [2,19]. In these experiments, the critical MC to sustain smouldering was 110% for IC of 3.7%, which is only 10% lower than the threshold in the model. Therefore, the model also successfully captures observed trends.

3.2. Simulating field-scale wildfire in Borneo

KAPAS was also used to study a real prescribed wildfire that took place on peatlands in Borneo, Indonesia in 2015. This fire was chosen because we obtained a fuel map and airborne footage of the fire from [25] (see Fig. A5). The field where the fire took place was 573 ha in size, equivalent to 416 x 620 cell grid in KAPAS, using the same cell size and time-step as mentioned in Section 2.3.

To simulate the Borneo wildfire, it was necessary to add 2 additional states to the model, representing 2 additional surface fuel types. These states were *dead surface vegetation (DV)* and *firebreak (FB)*. These were both similar to the regular *SV* state, but modified the base flame spread probability P_R . For the case of *DV* cells, P_R was multiplied by 1.12 following [18] for dead fuel (see appendix) which increases the spread rate, and for the case of *FB* cells,

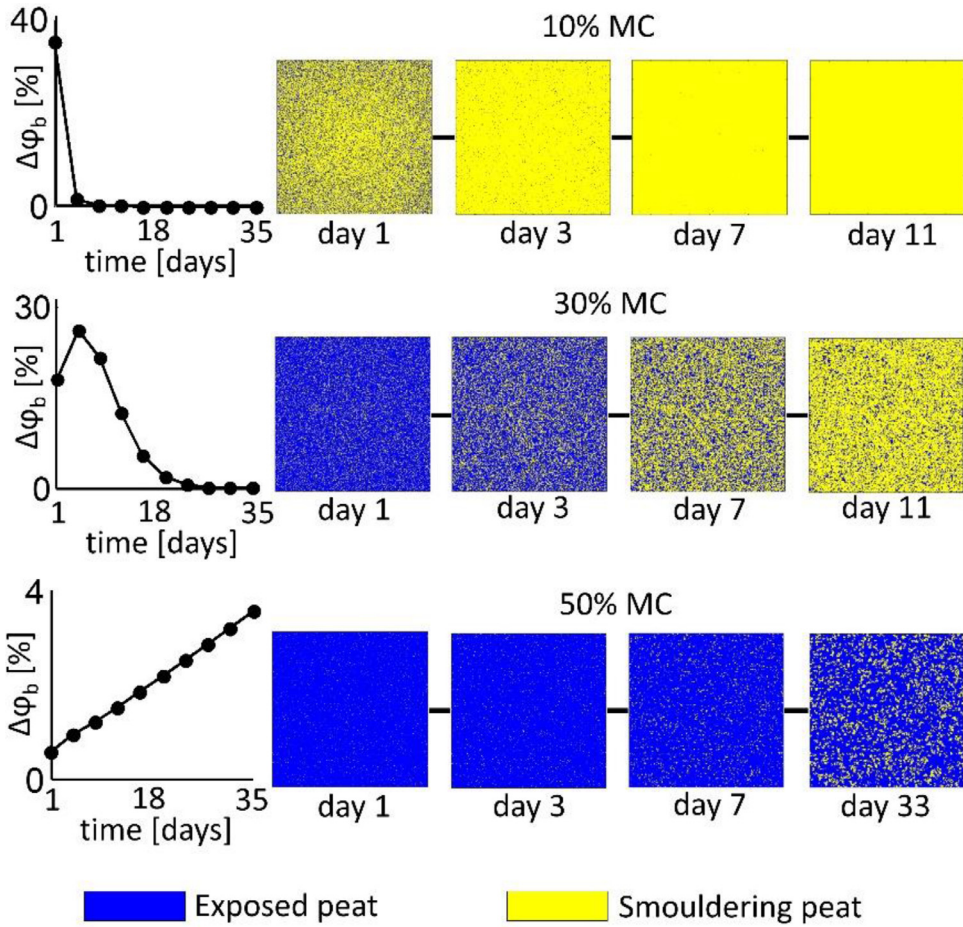


Fig. 4. Predicted $\Delta\phi_b$ with time and snapshots of the domain (400 x 400 cells) at different times and MC. $\Delta\phi_b$ is relative to the previous 3.5 day.

P_R was multiplied by 0 because firebreak are created to stop the spread of flaming wildfire by removing all surface vegetation on its area. These firebreak were only on the surface, therefore, smouldering fires could still spread.

The wind was taken from local measurements during the wildfire. The data was only available for the first day, therefore, the wind speed and direction was assumed to repeat the first day data over the following days. MC was varied from 0 to 150% in increments of 10%, which is representative of the change in MC between dry and rainy seasons in Indonesia and demonstrates a range of possible conditions during the fire. However, it is assumed that a typical value of MC in Indonesian peatlands is around 70% [20]. KAPAS was run for a total of 30,000 time-steps in this second case, which corresponds to a duration of 105 days in real time. This total duration is selected based on typical smoul-

dering peat wildfire duration in Indonesia which is around 2–3 months [24]. Only qualitative comparisons of the airborne footage with our simulations is possible because no other data is available publicly.

Figure 5 shows snapshots from the model with 70% MC at 4 different times for IC of 3.7%. The wind strength and direction are labelled in each snapshot, and δt is equal to the real time since ignition. In Fig. 5a, the surface vegetation has just been ignited. In 5b, at 13 h since ignition, the flaming front is halfway sweeping the surface layer and hotspots are formed. However, hotspots are not visible because they are too small for the figure resolution. In 5c, at 73 days since ignition, all of the peat has been exposed and hotspots are visible. In 5d, at 105 days since ignition, the hotspots are merging. By the end of the simulation, 2.9 ha of peat has burnt. The model captures the qualitative

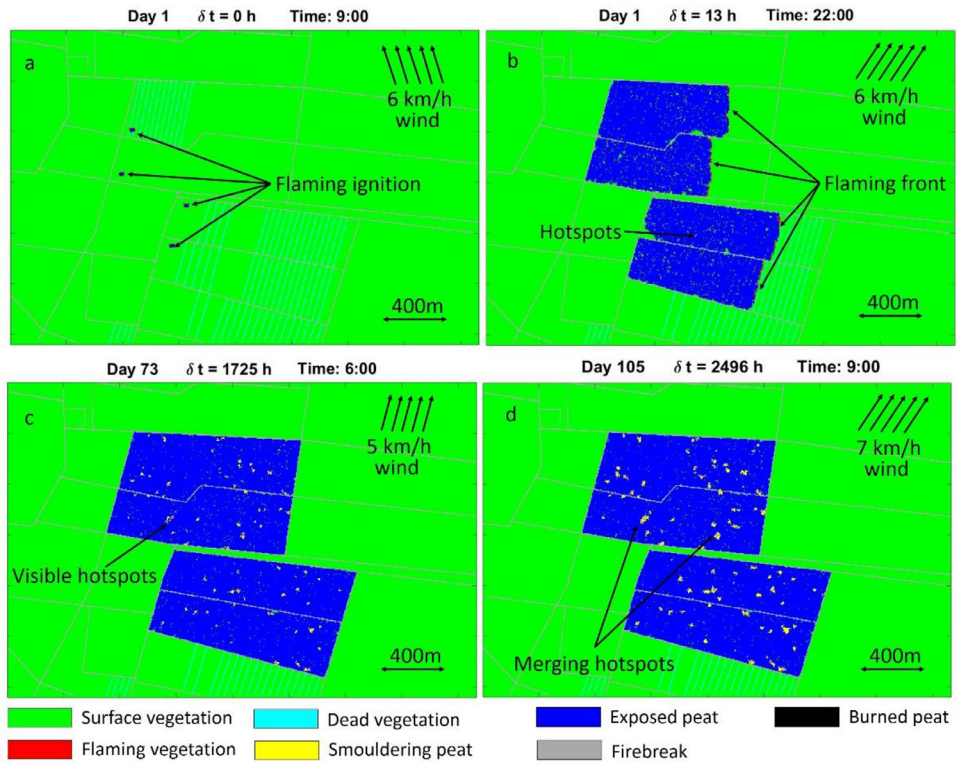


Fig. 5. Snapshots of a simulation of the prescribed fire in 573 ha (416 x 620 cells) of peatland in Borneo taken at different times (δt). (a) The start of the surface flaming, (b) the spread of surface flaming and the formation of smouldering hotspots, (c) the growth of smouldering, and (d) the merging of the smouldering hotspots.

behaviour seen during the wildfire of multiple hotspots igniting and then merging over time. The merging behaviour from KAPAS simulation is similar to the merging in the real peat wildfire shown in Fig A4. This result demonstrates the potential of cellular automata for modelling field-scale peat wildfires.

In the simulation at 70% MC, the flaming spread rapidly and reached the firebreak within less than 24 h. The peat that was ignited from this flaming took much longer to spread, and hotspots only became visible after 20 days. The hotspots continued to grow, spreading across firebreak, until 3 months when they began to merge. At this point, the burnt area became so large that suppressing the fire would be very difficult. Peat wildfires which remain active for months is a disastrous consequence of an unsafe prescribed fire on peatlands.

Figure 6 shows predicted burnt area (A_b) at different time after flaming ignition with increasing peat MC for IC of 3.7%. The line fitted through the blue circles represents A_b immediately after all surface vegetation has been consumed, which we refer to this as the *transition area*. The line fitted through the red diamonds represents the final A_b after 105 days. This is the *final burnt area*.

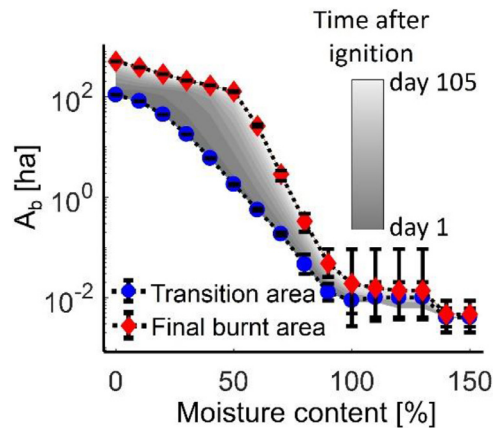


Fig. 6. Predicted A_b of the Borneo prescribed fire for different moisture content. The colour gradation represents change of A_b every 10 days. Each simulation is repeated 10 times to report uncertainty. (For interpretation of the references to colour in this figure, the reader is referred to the web version of this article.)

Figure 6 shows that the prescribed fire would have resulted in a smaller wildfire at higher MC, with less than 200 m² of peatland being burnt af-

ter 3 months if peat were above 100% MC. These results agree that prescribed fires should only take place when the MC of the peat is sufficiently high, in order to minimize the risk of smouldering.

Cellular automata predictions stem from the selection of the transition probability of each state, therefore, calibration against further experiments could improve the model significantly. The stochastic nature of the model makes the experiments of [19] suitable to calibrate the probabilities. Therefore, KAPAS could be improved when experiments similar to [19] are available for other phenomena in peat wildfires (e.g. extinction probability instead of ignition probability of those in [19]).

4. Conclusions

We used cellular automata for the first time to model field-scale peatland fires where both smouldering and flaming combustion are present. Considering simpler domains, our model KAPAS showed complex emergent behaviour that influenced the fire behaviour. We showed that in fires with multiple ignition points, smouldering hotspots merged over time, meaning the evolution of burnt area was non-linear. We found that both the transition ratio and final burnt ratio of smouldering peat followed a sigmoid relationship with moisture content, demonstrating key behaviour from the simple rules of the cellular automata and combining flaming and smouldering.

The model was also applied to a real peat wildfire that took place in Borneo in 2015 and managed to capture qualitative behaviour. At a realistic MC of 70%, 2.9 ha of peatland was burnt after 3 months. This burnt area could be reduced to a 150 times smaller area (0.02 ha) by increasing the MC above 100%, suggesting that prescribed fires should take place in conditions with high MC, such as during the wet season. These findings and model can improve the procedure of prescribed fires on peatlands, which is one way to help prevent the widespread occurrence of peat wildfires.

Declaration of Competing Interest

The authors declare that they have no known competing financial interests or personal relationships that could have appeared to influence the work reported in this paper.

Acknowledgements

This research was sponsored by European Research Council (ERC) Consolidator Grant HAZE (682587), and Indonesian Endowment Fund for Education (LPDP).

Supplementary material

Supplementary material associated with this article can be found, in the online version, at doi:[10.1016/j.proci.2020.08.052](https://doi.org/10.1016/j.proci.2020.08.052).

References

- [1] G. Rein, SFPE Handbook of Fire Protection Engineering, Springer, 2016, pp. 581–603, doi:[10.1007/978-1-4939-2565-0_19](https://doi.org/10.1007/978-1-4939-2565-0_19).
- [2] X. Huang, G. Rein, *Int. J. Wildland Fire* 24 (2015) 798–808, doi:[10.1071/WF14178](https://doi.org/10.1071/WF14178).
- [3] G. Rein, in: Fire Phenomena in the Earth System – An Interdisciplinary Approach to Fire Science, Wiley and Sons, 2013, pp. 15–34, doi:[10.1002/9781118529539.ch2](https://doi.org/10.1002/9781118529539.ch2).
- [4] T.A. Waldrop, S.L. Goodrick, *South. Res.* (2012).
- [5] B.D. Malamud, G. Morein, D.L. Turcotte, *Science* 281 (1998) 1840–1841, doi:[10.1126/science.281.5384.1840](https://doi.org/10.1126/science.281.5384.1840).
- [6] W.M. Block, L.M. Conner, P.A. Brewer, et al., *Md. USA Wildl. Soc. Tech. Rev.* (2016).
- [7] A. Noble, J. O'Reilly, D.J. Glaves, A. Crowle, P.S. M. J. Holden, *PLoS ONE* 13 (11) (2018), doi:[10.1371/journal.pone.0206320](https://doi.org/10.1371/journal.pone.0206320).
- [8] A.R. Harper, S.H. Doerr, C. Santin, C.A. Froyd, P. Sinnadurai, *Sci. Total Environ.* 624 (2018) 691–703, doi:[10.1016/j.scitotenv.2017.12.161](https://doi.org/10.1016/j.scitotenv.2017.12.161).
- [9] M.A. Santoso, E.G. Christensen, J. Yang, G. Rein, *Front. Mech. Eng.* 5 (49) (2019), doi:[10.3389/fmech.2019.00049](https://doi.org/10.3389/fmech.2019.00049).
- [10] S. Wolfram, *Nature* 311 (1984) 419–424, doi:[10.1038/311419a0](https://doi.org/10.1038/311419a0).
- [11] J. von Neumann, Urbana: University of Illinois Press, 1966.
- [12] S.G. Berjak, J.W. Hearne, *Ecol. Model.* 148 (2002) 133–151, doi:[10.1016/S0304-3800\(01\)00423-9](https://doi.org/10.1016/S0304-3800(01)00423-9).
- [13] I. Karafyllidis, A. Thanailakis, *Ecol. Model.* 99 (1997) 87–97, doi:[10.1016/S0304-3800\(96\)01942-4](https://doi.org/10.1016/S0304-3800(96)01942-4).
- [14] C. Favier, *Phys. Lett. A* 330 (5) (2004) 396–401, doi:[10.1016/j.physleta.2004.07.053](https://doi.org/10.1016/j.physleta.2004.07.053).
- [15] C.M. Belcher, J.M. Yearsley, R.M. Hadden, J.C. McElwain, G. Rein, *Proc. Natl. Acad. Sci. U.S.A.* 107 (52) (2010) 22448–22453, doi:[10.1073/pnas.1011974107](https://doi.org/10.1073/pnas.1011974107).
- [16] N. Fernandez-Anez, K. Christensen, V. Frette, G. Rein, *Phys. Rev. E* 99 (13) (2019) 023314, doi:[10.1103/PhysRevE.99.023314](https://doi.org/10.1103/PhysRevE.99.023314).
- [17] A. Alexandridis, D. Vakalis, C. Siettos, G. Bafas, *Appl. Math. Comput.* 204 (2008) 191–201, doi:[10.1016/j.amc.2008.06.046](https://doi.org/10.1016/j.amc.2008.06.046).
- [18] R.C. Rothermel, *A Mathematical Model for Predicting Fire Spread in Wildland Fuels*, USDA Forest Service, Washington, DC, 1972 Research Paper INT-115.
- [19] W.H. Frandsen, *Can. J. Forest Res.* 27 (1997) 1471–1477, doi:[10.1139/x97-106](https://doi.org/10.1139/x97-106).
- [20] R.W. Nusantara, R. Hazriani, U.E. Suryadi, in: Proceedings of the IOP Conference Series: Earth and Environmental Science, 2018, doi:[10.1088/1755-1315/145/1/012090](https://doi.org/10.1088/1755-1315/145/1/012090).
- [21] N. Prat-Guitart, G. Rein, R. Hadden, C. Belcher, J. Yearsley, *Int. J. Wildland Fire* 25 (4) (2016) 456–465, doi:[10.1071/WF15103](https://doi.org/10.1071/WF15103).

- [22] X. Huang, F. Restuccia, M. Gramola, G. Rein, *Combust. Flame* 168 (2016) 393–402, doi:[10.1016/j.combustflame.2016.01.017](https://doi.org/10.1016/j.combustflame.2016.01.017).
- [23] A. Usup, Y. Hashimoto, H. Takahashi, H. Hayasaka, *Tropics* 14 (2004) 1–19, doi:[10.3759/tropics.14.1](https://doi.org/10.3759/tropics.14.1).
- [24] H. Hayasaka, A. Usup, D. Naito, *Remote Sens. Basel* 12 (2020), doi:[10.3390/rs12122055](https://doi.org/10.3390/rs12122055).
- [25] W. Eyal, S. Moafi, J. Men, N. Czyz, N. Ahmed, *For. Archit.* (2017). [Online]. Available <https://forensic-architecture.org/investigation/ecocide-in-indonesia> .